Supporting Information

CdS nanofeathers enable efficient electron-mediator-free photocatalytic regeneration of coenzyme NAD(P)H via direct electron-proton coupling

Yao Chai,[a] Leyi Zhao,[a] Zirui Pang,[a] Liang Wan,[a] Heng Jiang,[a] Chi Chung Tsoi,[a] Yu Du,[a] Huaping Jia,[a] Yujiao Zhu,[a] Detao Liu,[d] Mingjie Li,[a] Fengjia Xie,[*a] Guangya Zhou[*c] and Xuming Zhang[*ab]

[a]Department of Applied Physics, The Hong Kong Polytechnic University, Hong Kong, China.
[b]Research Centre for Resources Engineering towards Carbon Neutrality (RCRE), The Hong Kong Polytechnic University, Hong Kong, China.
[c]Department of Mechanical Engineering, National University of Singapore, Singapore, Singapore.
[d]School of Light Industry and Engineering, South China University of Technology, Guangzhou, China.

Correspondence to: xuming.zhang@polyu.edu.hk

CONTENTS

Raw Materials.

Cadmium chloride hemi(pentahydrate) ($CdCl_2 \cdot 2.5H_2O$, 79.5-81.0%), Thiourea (NH_2CSNH_2, ≥99.0%), β-Nicotinamide adenine dinucleotide hydrate (NAD^+, ≥99%), β-Nicotinamide adenine dinucleotide, reduced disodium salt hydrate (β-NADH, ≥97%), β-Nicotinamide adenine dinucleotide phosphate hydrate (β-$NADP^+$, ≥95%), Pentamethylcyclopentadienylrhodium(III) chloride dimer [$(Cp^*RhCl_2)_2$, ≥97%], Ethylene Glycol ($HOCH_2CH_2OH$, ≥99%), and 2, 2'-Bipyridyl ($C_{10}H_8N_2$, ≥99%) were purchased from Sigma-Aldrich Chemical Reagent Co., Ltd.

Synthesis of $[Cp^*Rh(bpy)H_2O]^{2+}$ electron mediator.

The synthesis method of $[Cp^*Rh(bpy)H_2O]^{2+}$ adheres to a previously reported procedure. Initially, 0.1 mmol of $(Cp^*RhCl_2)_2$ and 0.2 mmol of 2,2'-bipyridine are added to 4 mL of methanol and stirred until dissolved. Once the solution naturally evaporates to about 1 mL, 40 mL of cold ether is quickly added to precipitate $[Cp^*Rh(bpy)Cl]Cl$. After filtering the ether, 8 mL of deionized water is added to obtain $[Cp^*Rh(bpy)H_2O]^{2+}$. The $[Cp^*Rh(bpy)H_2O]^{2+}$ solution is then stored at 8°C in the dark for future use as an electron mediator in the photocatalytic regeneration of NAD(P)H.

Characterization.

The crystal structure of the catalyst is analyzed using an X-ray powder diffractometer (XRD, Rigaku SmartLab X-ray diffractometer). The micromorphology and crystal structure of the photocatalyst are observed with a transmission electron microscope (TEM, FEI TS12). The chemical composition of the photocatalyst samples is characterized by X-ray photoelectron spectroscopy (XPS, Thermo ESCALAB 250XI). The collected data are corrected to eliminate the charging effect using the binding energy of the substrate C 1s peak (284.8 eV). The electron paramagnetic resonance spectrum (EPR) is measured on a Bruker A-300-EPR spectrometer. The ultraviolet-visible (UV-vis) diffuse reflectance spectrum is measured using a PerkinElmer UV-vis-NIR spectrometer with an integrating sphere, with a scanning range set to 250–800 nm and a measurement rate of 2 nm/s. The photoluminescence (PL) spectrum and time-resolved photoluminescence (TRPL) spectrum are obtained on an Edinburgh fluorescence spectrometer (PLS1000). For femtosecond laser pulse excitation measurements, a Ti laser (Coherent Libra) is used as the excitation source to generate femtosecond pulses (50 fs, 1 kHz) at an emission wavelength of 800 nm. The transient absorption spectra are measured by an ultrafast HELIOS TA system, where a pump beam of 340 nm (~200 μW) fs laser excites the sample. The probe beam is focused at the center of the pump beam (2 mm diameter) on the sample.

Photocurrent and electrochemical impedance measurements.

The CHI660 electrochemical workstation is used for photoelectric performance testing. The working electrode is prepared as follows: 10 mg of the photocatalyst is dispersed in 1 mL of ethanol, 20 μL of 5% Nafion solution is added, and ultrasonic dispersion is performed. 20 μL of the resulting dispersion is dropped onto a 1 cm^2 conductive glass surface and air-dried. For photocurrent measurement, a Pt plate is used as the counter electrode, Ag/AgCl is used as the reference electrode, and a 0.2 M Na_2SO_4 solution is used as the electrolyte. For electrochemical impedance measurement, the open circuit voltage is used as the initial voltage, and the frequency range is 0.01 Hz to 100 kHz. A 0.5 M KCl solution and a 5.0 mM $K_3[Fe(CN)_6]/K_4[Fe(CN)_6]$ solution are used as electrolytes.

Calculation of photon numbers

The formula for calculating the number of incident photons of monochromatic light is as follows

$$N_{\text{Photonnumber}} = \frac{I \times S \times \lambda \times t}{hc}$$

I: Light intensity (W m^{-2}), S: Illumination area S ≈ 0.015 × 0.01 (m^{-2}), λ: Monochromatic light wavelength (m), t: Light time (s), h: Planck's constant (6.626×10^{-34}), c: Speed of light (3×10^{8} m s^{-1}).

Theoretical Calculations.

The electron exchange and correlation were described with GGA-RPBE functional[1,2]. The localized double-numerical quality basis set with a polarization d-function (DNP-4.4 file) was chosen to expand the wave functions[3]. The core electrons of the metal atoms were treated using the effective core potentials (ECP)[3,4], and the orbital cutoff was 4.5 Å for all atoms. For the geometry optimization, the convergences of the energy, maximum force, and maximum displacement were set as 2×10^{-5} Ha, 4×10^{-3} Ha/Å, and 5×10^{-3} Å, and the SCF convergence for each electronic energy was set as 1.0×10^{-5} Ha. The vibrational frequency analysis was performed to gain the thermodynamic results. According to the vibrational analysis, the correlation of thermodynamic parameters (with the zero-point energy included) of the free energy (ΔG_{corr}) was taken into consideration in the study of the reaction mechanism[5]. And the free energy at specific temperature were calculated by the formula $G = E_{total} + G_{corr}$, where E_{total} is the total energy of the specific molecular and G_{corr} is the free energy correlation with the zero-point energy included at the specific temperature. So, the related free energy change at 298.15 K in each step was obtained by using the equation $\Delta G = \Delta E_{total} + \Delta G_{corr}$, where ΔE_{total} is the energy difference of the total energy between each species, and ΔG_{corr} is the energy difference of the free energy correlations at 298.15 K.

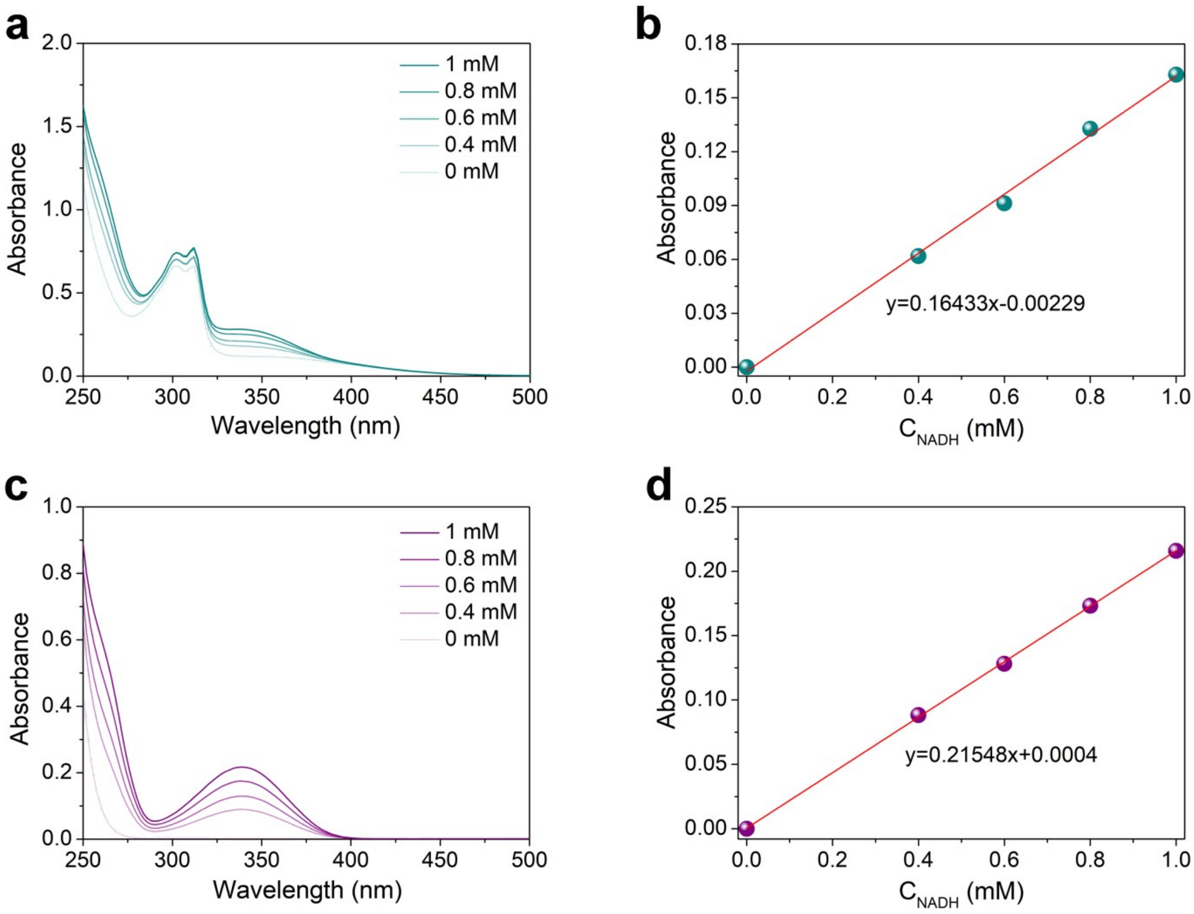

Fig. S1 (a) UV-visible absorption spectra of of NADH at different concentrations in an environment containing an electron mediator and (b) the corresponding standard curve. (c) UV-visible light absorption spectra of NADH at different concentrations in an environment without electron mediator and (d) the corresponding standard curve.

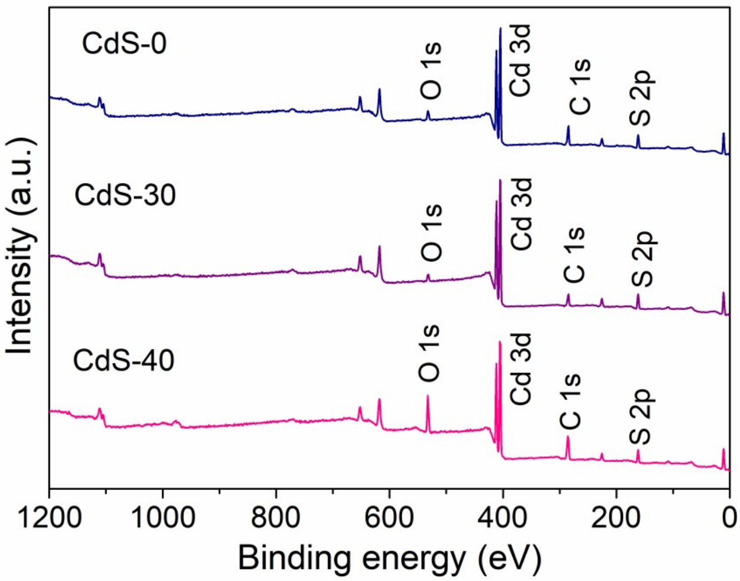

Fig. S2 XPS full spectra of CdS-0, CdS-30, and CdS-40 samples.

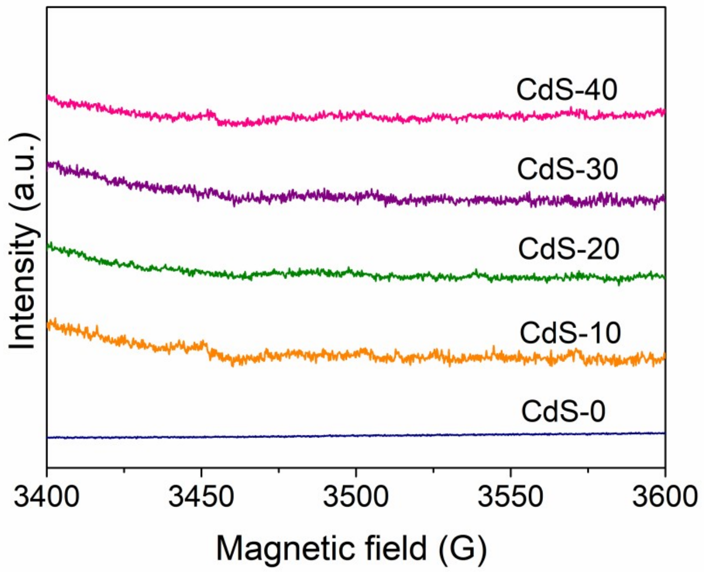

Fig. S3 EPR spectra of a series of photocatalysts.

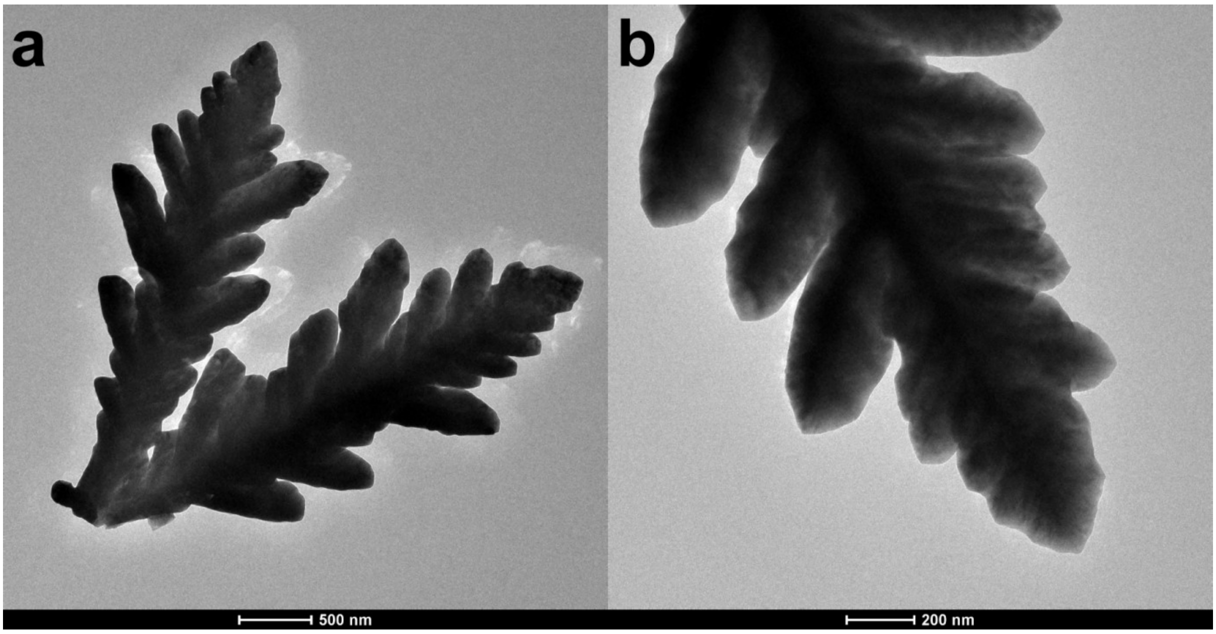

Fig. S4 TEM images of CdS-0 samples at various magnifications.

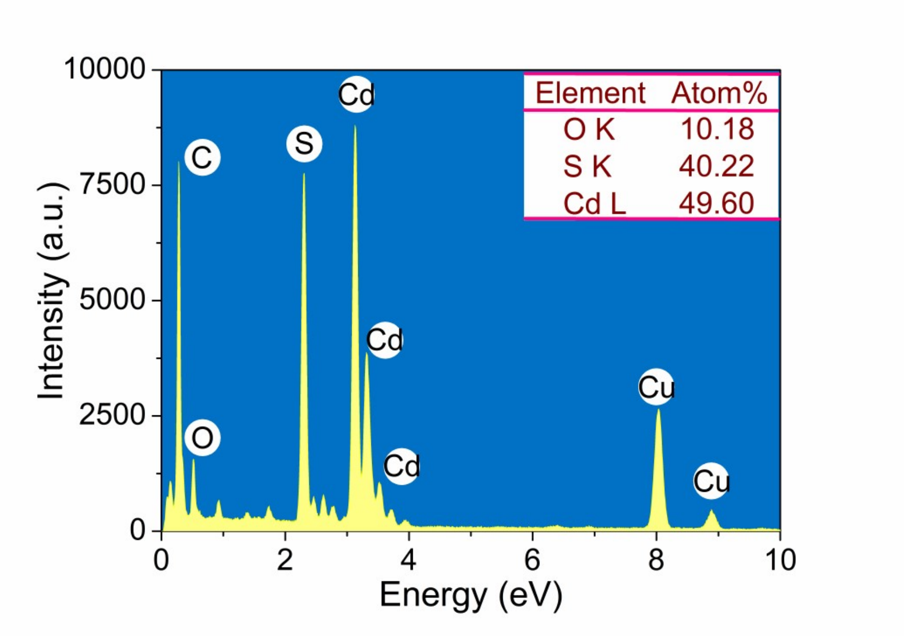

Fig. S5 Typical EDS spectrum of the CdS-30 sample.

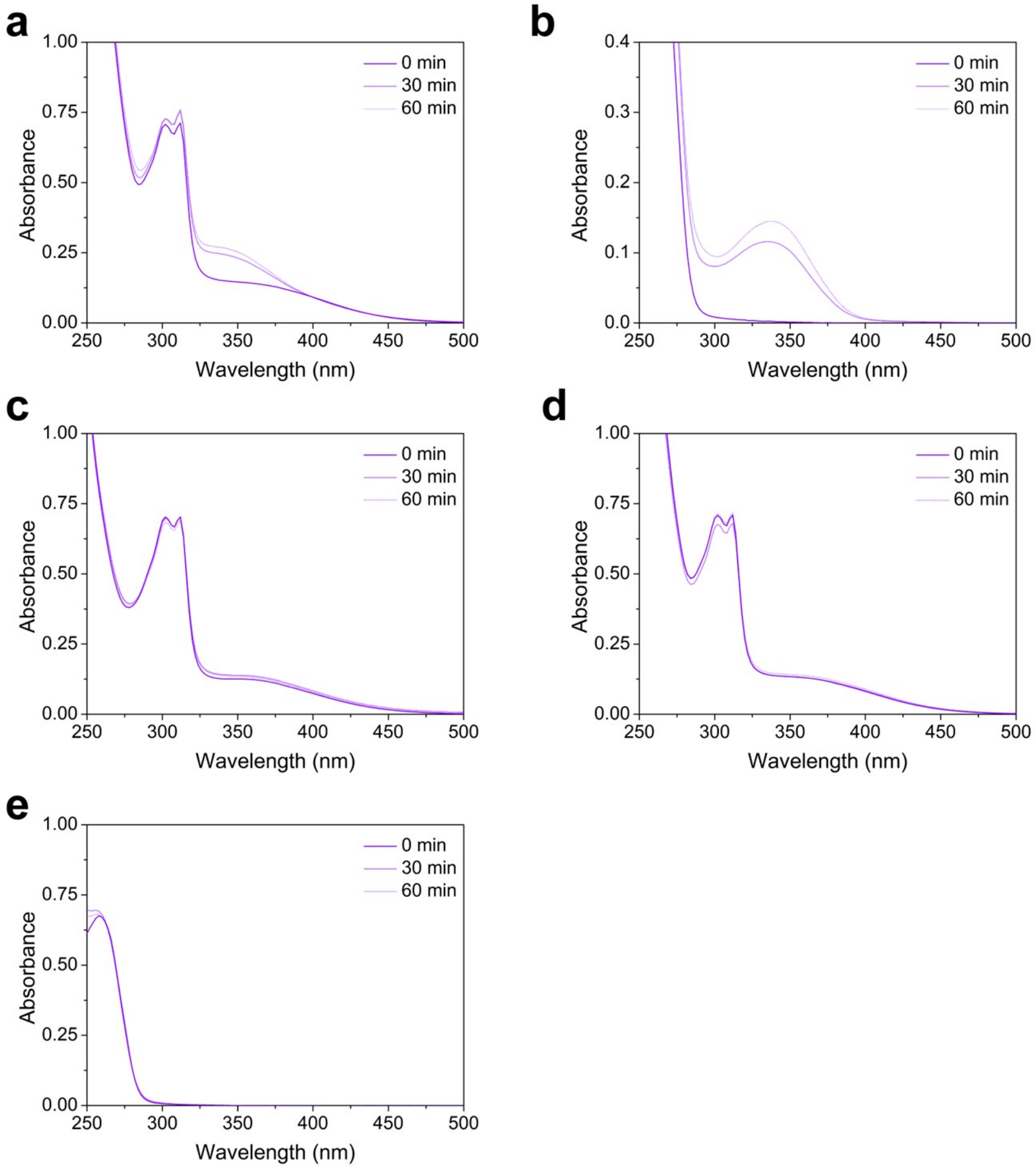

Fig. S6 Time-resolved UV-visible absorption spectra from a series of control experiments on the regeneration of the photocatalytic coenzyme NADH. (a) Normal reaction. (b) Without electron mediator. (c) Without NAD$^+$. (d) Without photocatalyst. (e) Without triethanolamine.

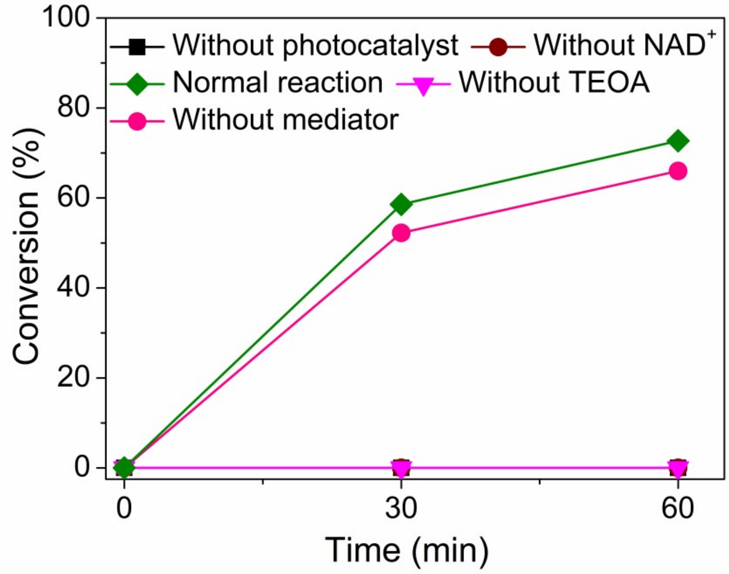

Fig. S7 A series of controlled experiments.

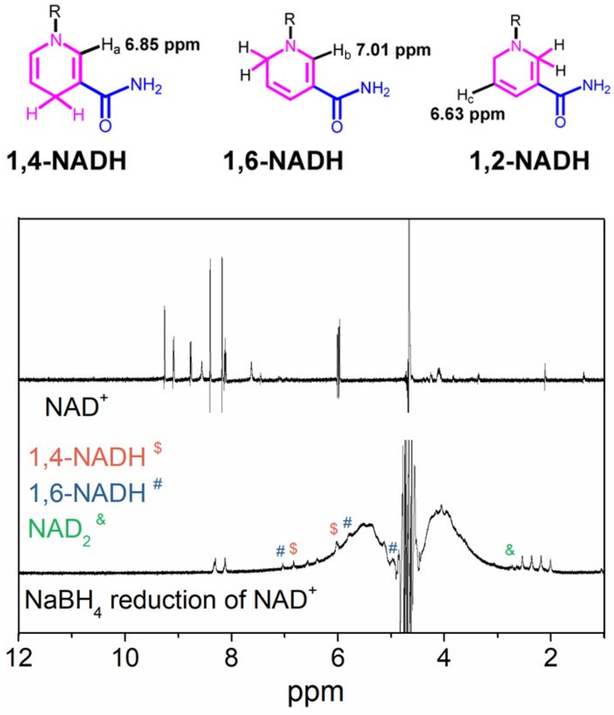

Fig. S8 ^{1}H NMR spectrum of NADH isomers generated via NaBH$_4$ reduction of NAD$^+$.

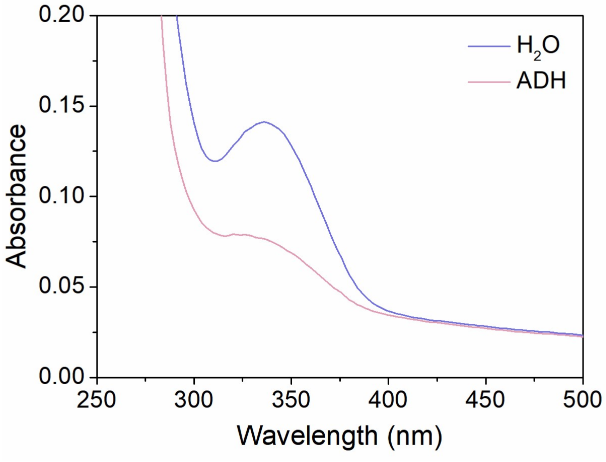

Fig. S9 UV-Vis spectra of NADH consumption as a product of enzymatic photoreduction.

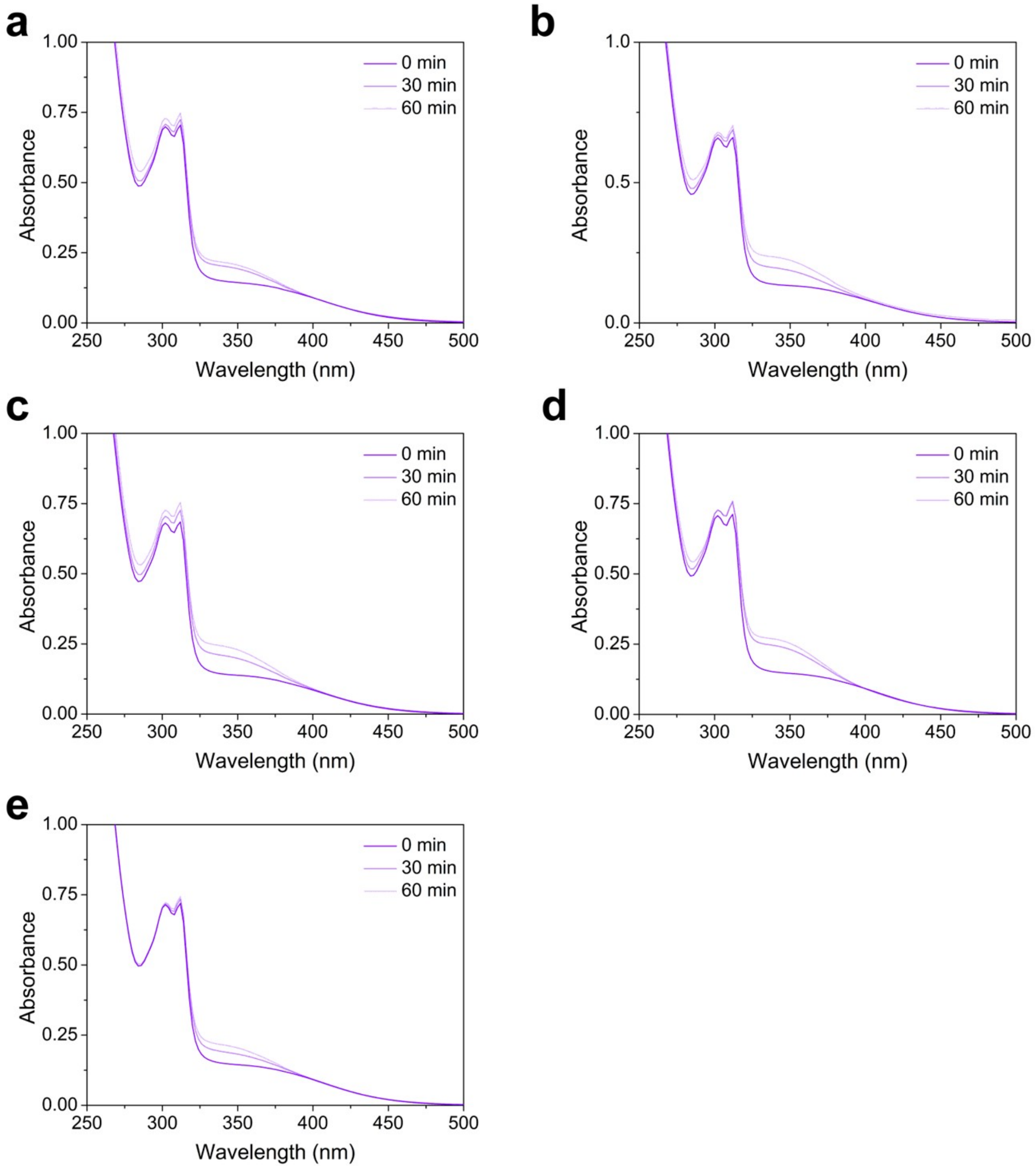

Fig. S10 Time-resolved UV-visible absorption spectra of a series of CdS photocatalysts for photocatalytic regeneration of coenzyme NADH with the assistance of electron mediators. (a) CdS-0, (b) CdS-10, (c) CdS-20, (d) CdS-30, and (e) CdS-40.

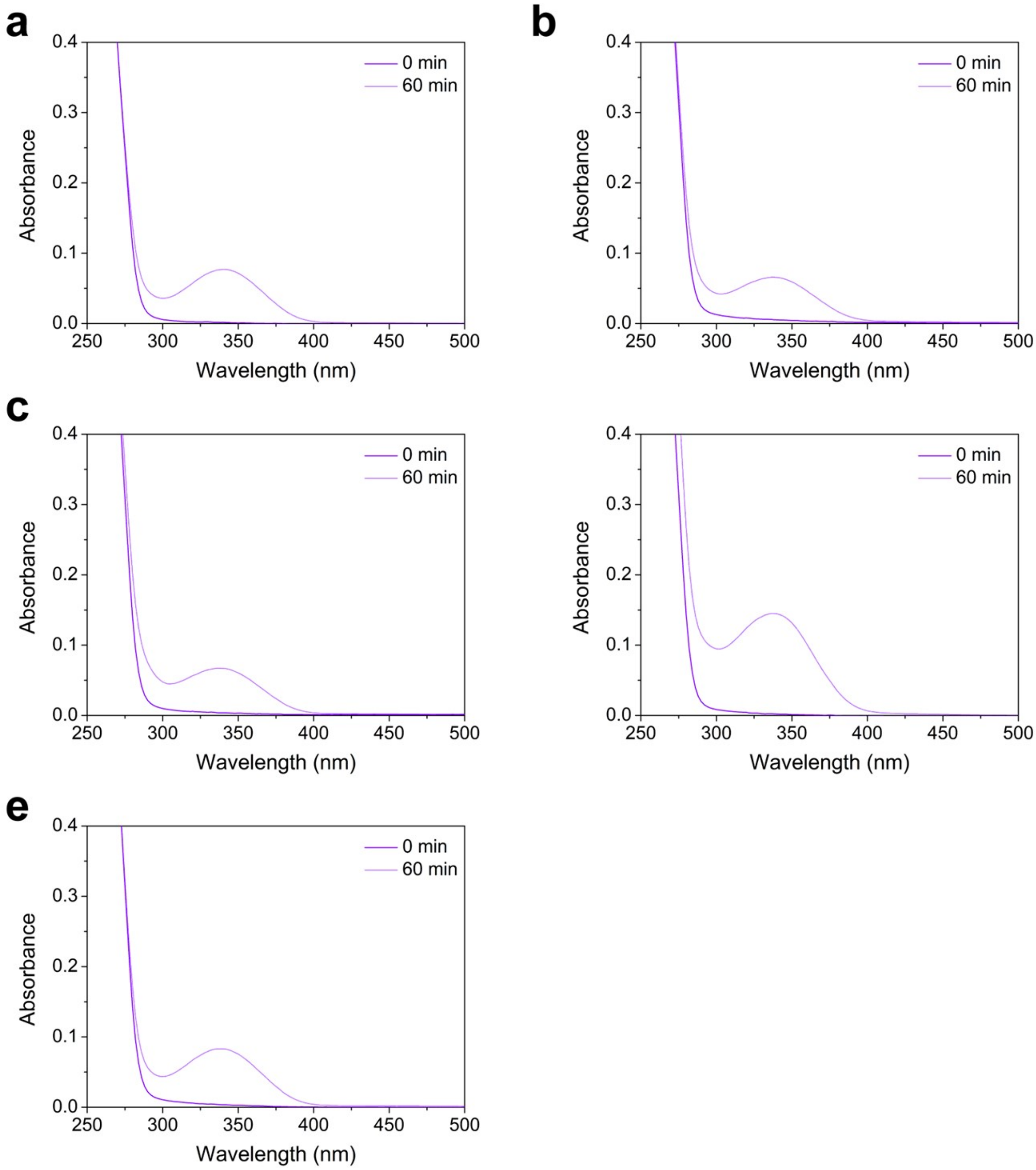

Fig. S11 Time-resolved UV-visible absorption spectra of a series of CdS photocatalysts for photocatalytic regeneration of coenzyme NADH in the absence of electron mediators. (a) CdS-0, (b) CdS-10, (c) CdS-20, (d) CdS-30, and (e) CdS-40.

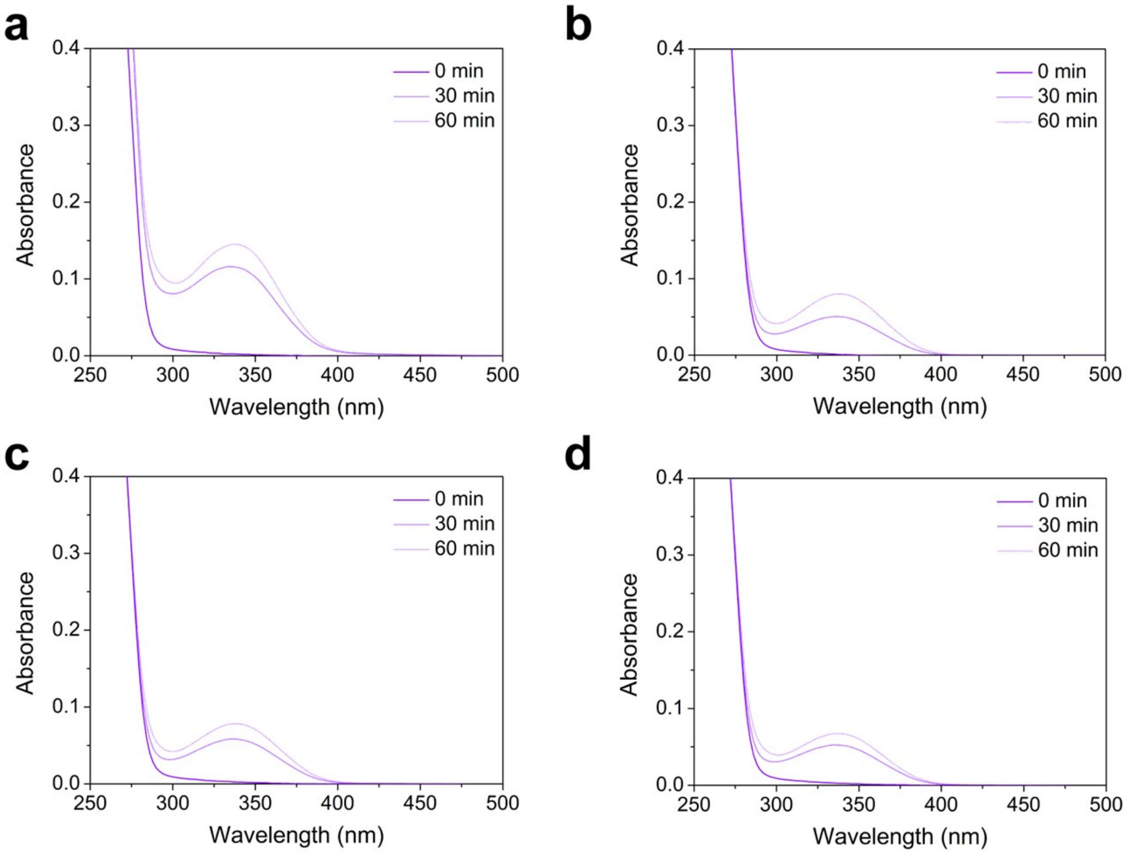

Fig. S12 Time-resolved UV-visible absorption spectra of coenzyme NADH regeneration by CdS-30 under different monochromatic light without an electron mediator. (a) ≥420 nm, (b) 420 nm, (c) 450 nm, and (d) 475 nm.

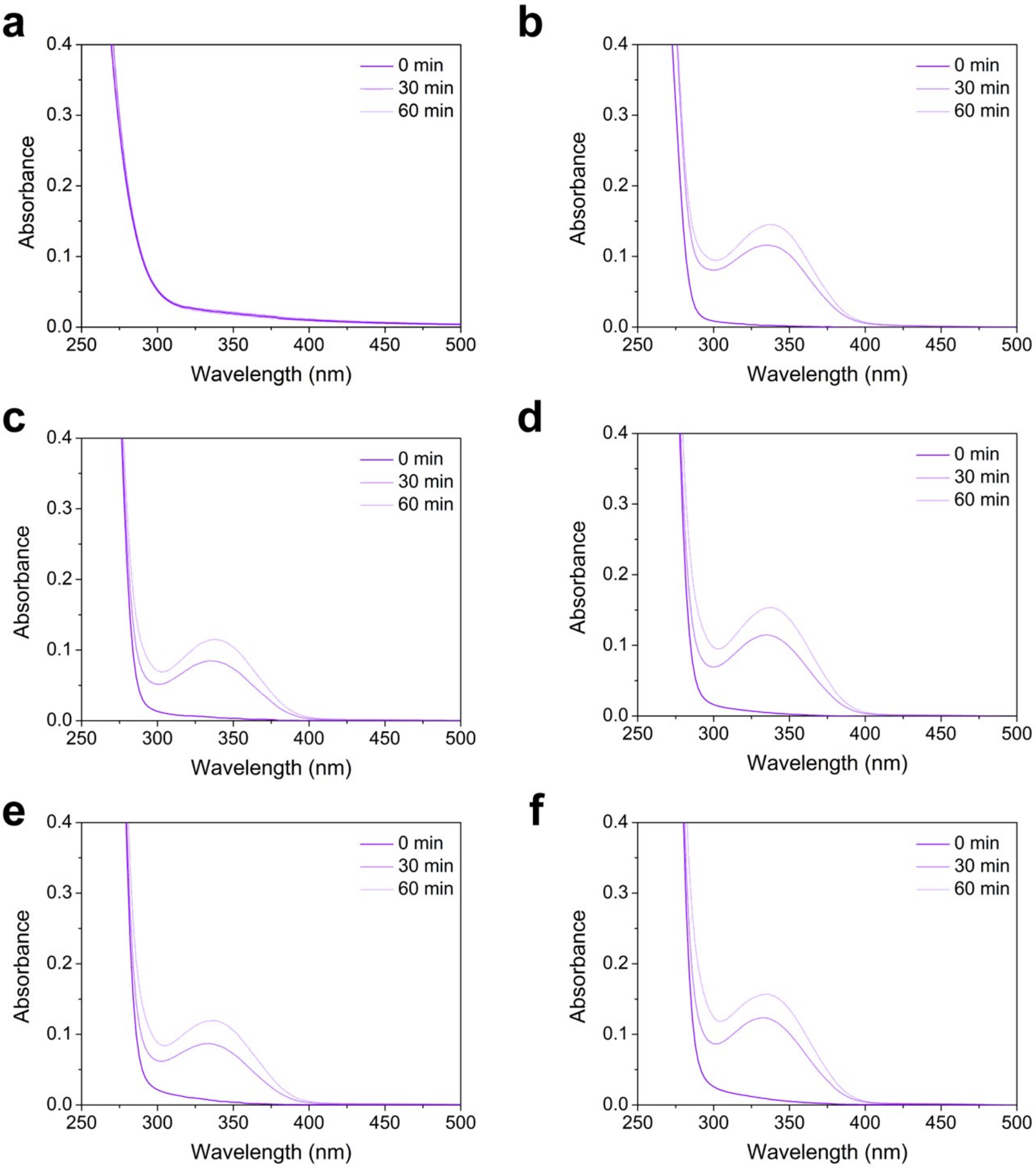

Fig. S13 Time-resolved UV-visible absorption spectra of NAD⁺ solutions with different initial concentrations on the photocatalytic regeneration of coenzyme NADH over CdS-30. (a) 0 mM, (b) 0.250 mM, (c) 0.375 mM, (d) 0.500 mM, (e) 0.625 mM, and (f) 0.750 mM.

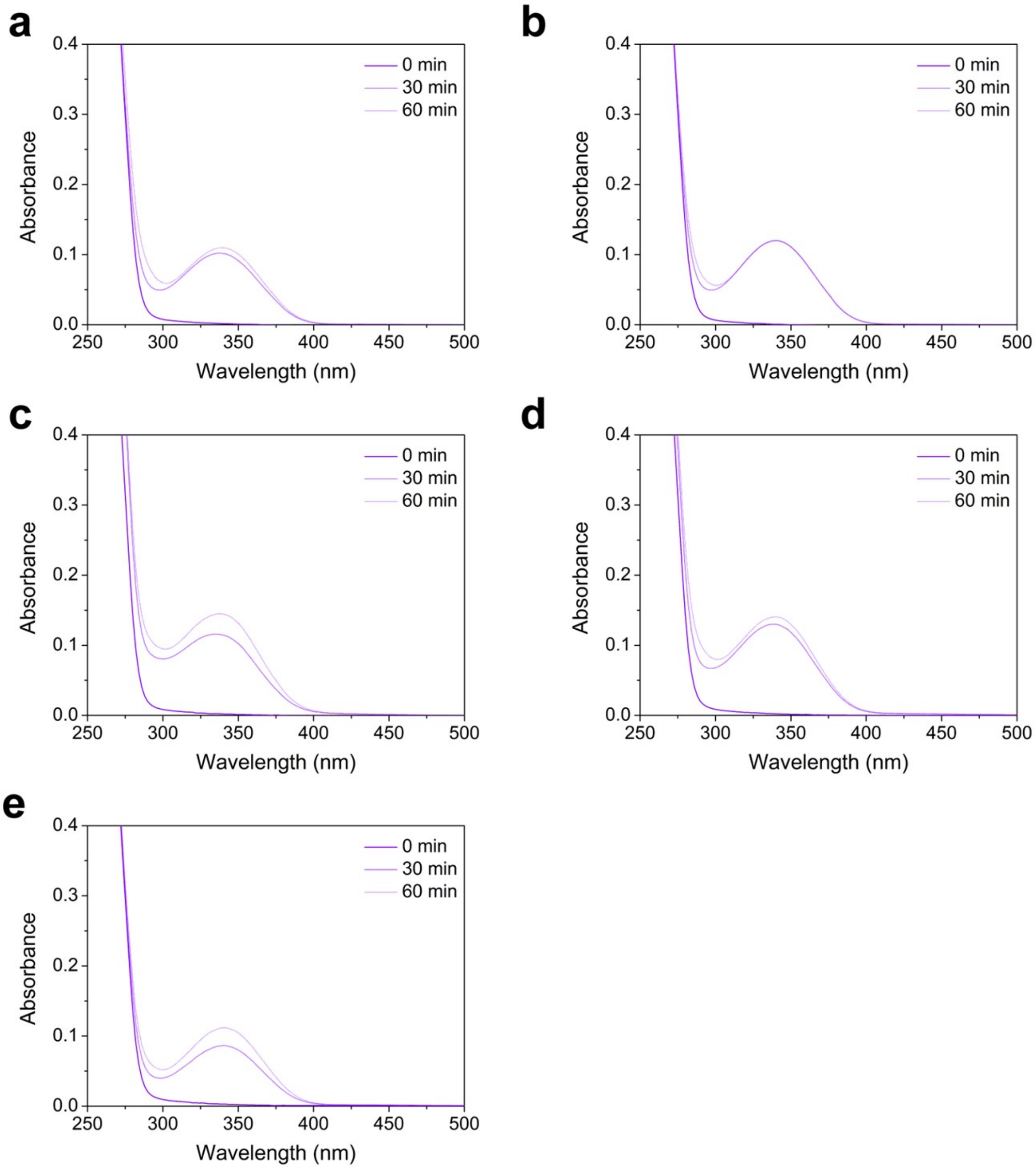

Fig. S14 Time-resolved UV-visible absorption spectra of five cycles of photocatalytic regeneration of coenzyme NADH on CdS-30. (a) First time, (b) Second time, (c) Third time, (d) Fourth time, and (e) Fifth time.

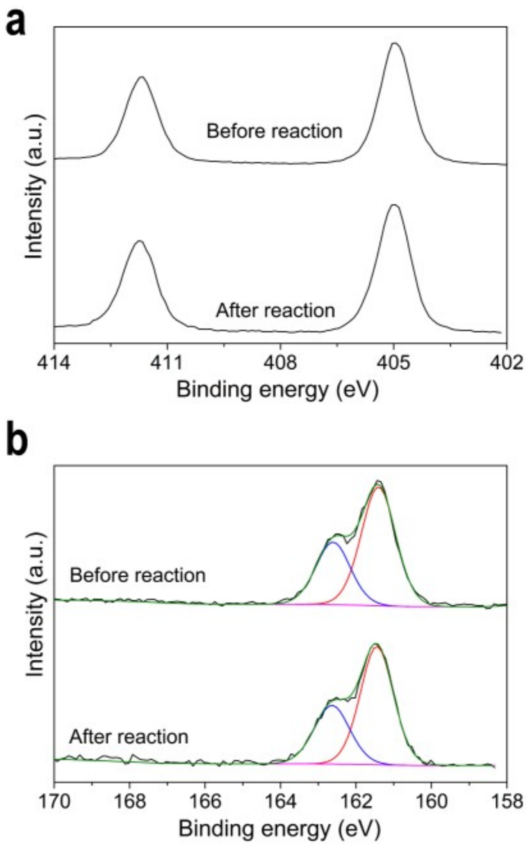

Fig. S15 XPS spectra of the catalyst before and after the reaction. (a) Cd *3d*, (b) S *2p.*

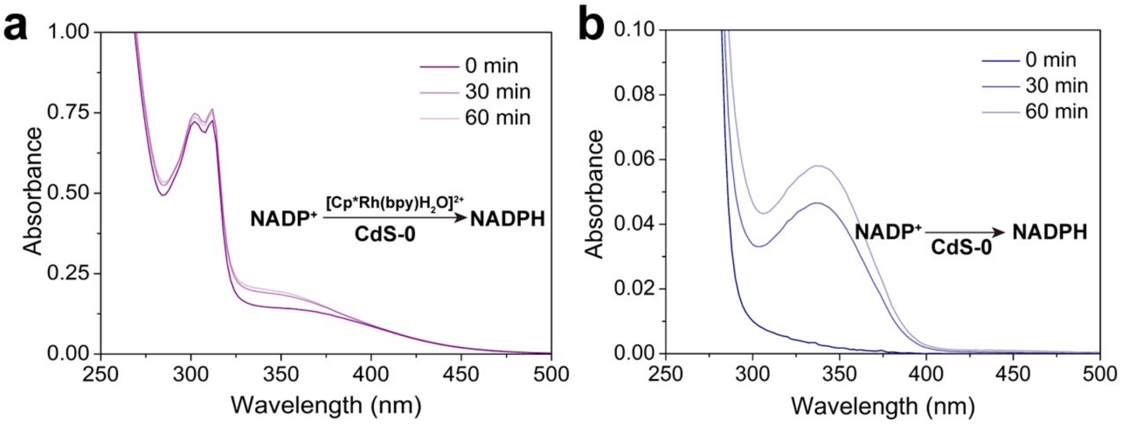

Fig. S16 (a, b) Photocatalytic coenzyme NADPH regeneration of CdS-0 with and without electron mediator.

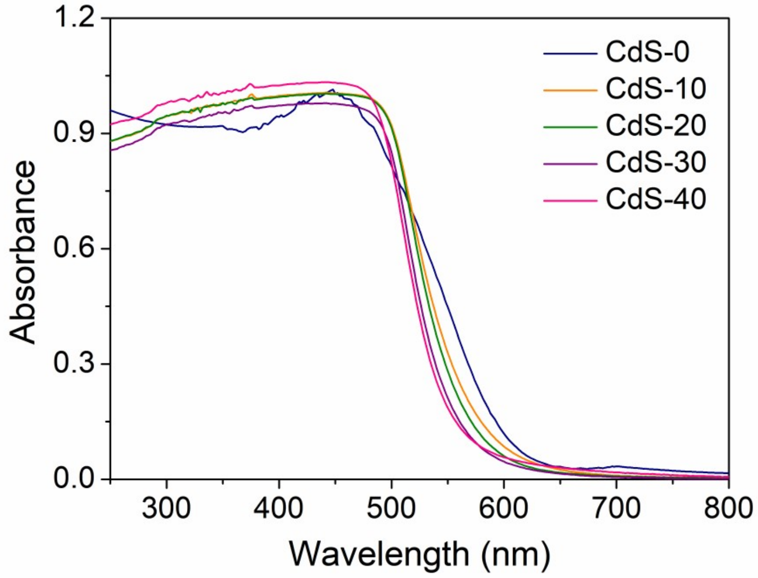

Fig. S17 UV-Vis absorption spectra of a series of photocatalysts.

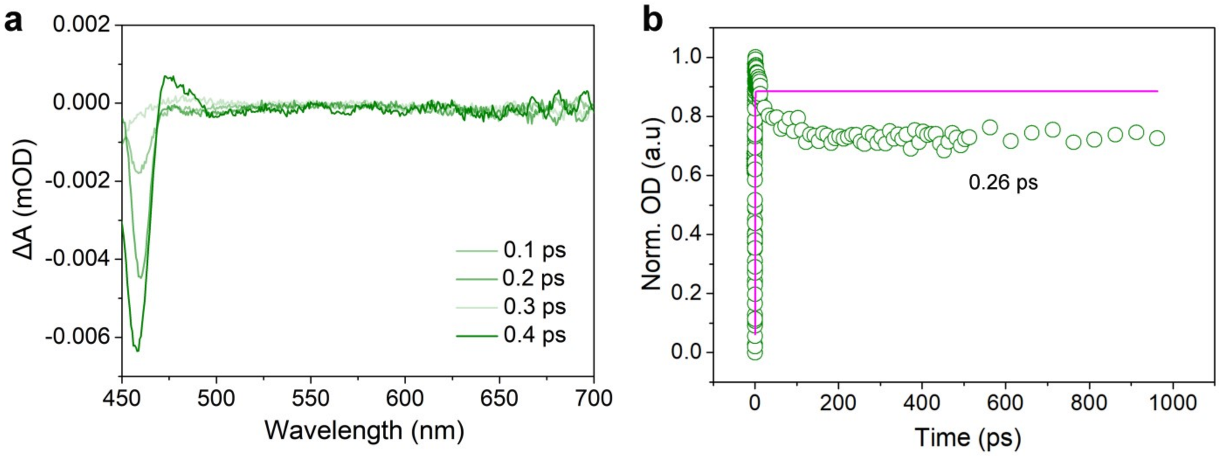

Fig. S18 (a) Transient absorption spectra of CdS-30 at various delay times under 400 nm excitation after adding TEOA. (b) Kinetics of CdS-30 probed at 460 nm after adding TEOA.

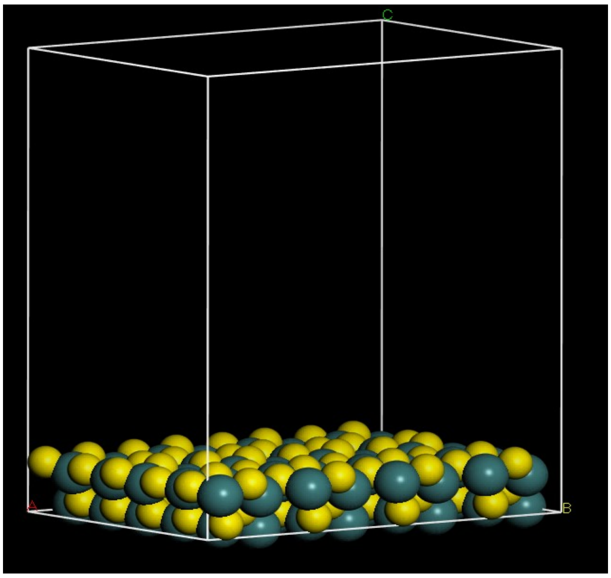

Fig. S19 CdS (1 0 1) crystal plane.

Table S1. Comparative assessment of the photocatalytic NADH regeneration performance between CdS-30 sample and conventional photocatalysts.

Catalyst	**Reaction time**	**Electron donor**	**$[Cp^*Rh(bpy)H_2O]^{2+}$**	**NAD^+ conversion rate (%)**	**Ref.**
CdS-30	1 h	TEOA	Yes	72.7	This work
CdS-30	1 h	TEOA	/	66.0	This work
N3-GDY	3 h	TEOA	Yes	35	6
TPPS/Cd aggregates	3h	TEOA	/	60	7
TCM-15%	0.5 h	TEOA	/	46	8
PDI/CN hybrid	3 h	TEOA	Yes	75	9
CN	3 h	TEOA	Yes	52	9
QDs@Flake g-C_3N_4	4 h	TEOA	Yes	40	10
QDs@Flake g-C_3N_4	4 h	TEOA	/	22.5	10
ART72	50 min	EDTA-2Na	Yes	29	11
P25-TiO_2	50 min	EDTA-2Na	Yes	42	11
ARTM36	50 min	EDTA-2Na	Yes	76	11
ARTM36	50 min	LA	Yes	49	11
ARTM36	50 min	TEOA	Yes	39	11
ARTM36	50 min	EDTA-2Na	/	65	11
RF@PANI	3 h	TEOA	Yes	68.02	12
RF	3 h	TEOA	Yes	~17	12

TPTTA$_5$@TPBpy$_{0.5}$-Rh/SiO$_2$	40 min	TEOA	/	47	13
TPTTA$_5$@TPBpy$_{1.5}$-Rh/SiO$_2$	40 min	TEOA	/	58	13
Ti$_3$C$_2$	5 h	TEOA	/	14.68	14
COF-367	5 h	TEOA	/	60.97	14
10% Ti$_3$C$_2$/COF-367	5 h	TEOA	/	83.38	14

References

1. J. Kim, T. Lee, H. D. Jung, M. Kim, J. Eo, B. Kang, H. Jung, J. Park, D. Bae, Y. Lee, S. Park, W. Kim, S. Back, Y. Lee, D. H. Nam, *Nat. Commun.*, 2024, **15**, 192.
2. B. Deng, Z. Chen, L. Yang, J. Guo, C. Cheng, X. Li, S. Zhang, S. Luo, *J. Hazard. Mater.*, 2024, **466**, 133606.
3. F. Fan, Z. Chen, A. Zhou, Z. Yang, Y. Zhang, X. He, J. Kang, W. Zhou, *Fuel*, 2023, **333**, 126351.
4. C. Liao, J. M. Kasper, A. J. Jenkins, P. Yang, E. R. Batista, M. J. Frisch, X. Li, *JACS Au*, 2023*,* **3**, 358–367.
5. Y. Pan, Y. Chen, K. Wu, Z. Chen, S. Liu, X. Cao, W. C. Cheong, T. Meng, J. Luo, L. Zheng, C. Liu, D. Wang, Q. Peng, J. Li, C. Chen, *Nat. Commun.*, 2019, **10**, 4290.
6. Q. Pan, H. Liu, Y. Zhao, S. Chen, B. Xue, X. Kan, X. Huang, J. Liu, Z. Li, *ACS Appl. Mater. Interfaces*, 2019, **11**, 2740–2744.
7. L. Xiu, L. Zhang, X. Du, H. Cao, D. Wang, Y. Hu, Y. Qiao, Y. Ma, Y. Xia, S. Wang, *ACS Sustainable Chem. Eng.*, 2024, **12**, 2656–2667.
8. P. Wei, J. Dong, X. Gao, L. Chang, Z. Huang, H. Zheng, S. M. Y. Lee, W. Y. Lou, C. Peng, *ACS Sustainable Chem. Eng.*, 2024, **12**, 6881–6893.
9. Zhang, P. Hu, J. Shen, Y. Yang, X. Qu, J. Du, F. Sun, W. Li, C. M. *ACS Appl. Mater. Interfaces*, 2021, **13**, 46650–46658.
10. Yang, D. Zou, H. Wu, Y. Shi, J. Zhang, S. Wang, X. Han, P. Tong, Z. Jiang, Z. *Ind. Eng. Chem. Res.*, 2017*,* **56**, 6247–6255.
11. P. Wei, Y. Zhang, J. Dong, Y. Cao, S. M. Y. Lee, W. Lou, C. Peng, *Appl Catal B-Environ.*, 2024, **327**, 124257.
12. L. Zhou, Z. Su, J. Wang, Y. Cai, N. Ding, L. Wang, J. Zhang, Y. Liu, J. Lei, *Appl Catal B-Environ.*, 2024, **341**, 123290.
13. J. Liu, X. Ren, C. Li, M. Wang, H. Li, Q. Yang, *Appl Catal B-Environ.*, 2022, **310**, 121314.
14. J. Qu, T. Yang, P. Zhang, F. Yang, Y. Cai, X. Yang, C. M. Li, J. Hu, *Appl Catal B-Environ.*, 2024, **348**, 123827.